HHS Public Access

Author manuscript

ACS Sens. Author manuscript; available in PMC 2017 January 05.

Published in final edited form as:

ACS Sens. 2016 August 26; 1(8): 975–978. doi:10.1021/acssensors.6b00396.

pH-Dependent Cellular Internalization of Paramagnetic Nanoparticle

Branislava Janic[†], **Mohammed Pl. Bhuiyan**[‡], **James R. Ewing**[‡], and **Meser M. Ali**[‡,*]

[†]Radiation Oncology, Henry Ford Hospital, Detroit, MI 48202, United States

[‡]Department of Neurology, Henry Ford Hospital, Detroit, MI 48202, United States

Abstract

A hallmark of the tumor microenvironment in malignant tumor is extracellular acidosis, which can be exploited for targeted delivery of drugs and imaging agents. A pH sensitive paramagnetic nanoaparticle (NP) is developed by incorporating GdDOTA-4AmP MRI contrast agent and pHLIP (pH Low Insertion Peptide) into the surface of a G5–PAMAM dendrimer. pHLIP showed pH-selective insertion and folding into cell membranes, but only in acidic conditions. We demonstrated that pHLIP-conjugated Gd_{44}-G5 paramagnetic nanoparticle binds and fuses with cellular membrane at low pH, but not at normal physiological pH, and that it promotes cellular uptake. Intracellular trafficking of NPs showed endosomal/lysosomal path ways.

Graphical Abstract

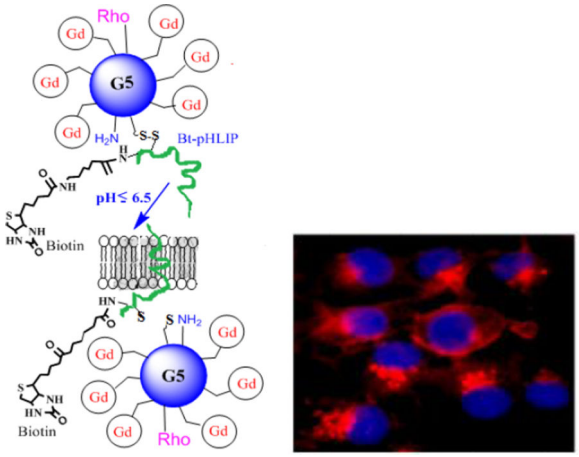

Keywords

Cell internalization; intracellular trafficking; paramagnetic nanoparticle; pH sensing probe; MRI

Corresponding Author. mali8@hfhs.org, Department of Neurology, Henry Ford Hospital, Detroit, MI 48202, United States.

ASSOCIATED CONTENT

Supporting Information

Supporting Information Available: The following files are available free of charge.

Experimental procedures, Conjugation of pHLIP and dye with nanoparticle, zeta potential and fluorescence imaging.

Overexpressed receptors and enzymes in cancer cells have received primary consideration as biomarkers for targeted imaging and/or therapy.[1] The variability of the cells in many human cancers, however, may limit approaches based on targeting specific cancer cell receptors.[2] Recent gene expression studies in cancer cells have demonstrated that many molecules, including various receptors are up- or down-regulated in individual tumor cells, resulting heterogeneous cell surfaces.[3] Therefore, progress for therapeutic tumor targeting is hampered by the diverse and heterogeneous nature of cancer, and relying on any single tumor biomarker for even one type of cancer can be problematic.

Recently, new targeting strategies have emerged as a way of improving the targeting efficiency of nanocarriers. These strategies utilize the unique microenvironment[4–6] of tumor cells, i.e. “tumoral extracellular environment,” as a molecular cue for activating long-circulating nanocarriers to release the drug or facilitate their cellular uptake upon arrival at the targeted tumor sites. These considerations lead to physiological markers of tumors as a focus for both detection and treatment.[5,6,7]

The tumor microenvironment is frequently characterized by an acidic extracellular pH_e and a neutral-to-alkaline intracellular pH_i.[8–10] This kind of pH gradient is not observed in normal tissues and blood.[11] An acidic tumor pH_e is caused by an increase glycolysis in tumor cells, which generates increased extracellular levels of bi-carbonate under aerobic conditions,[12,13] or lactic acid under anaerobic conditions.[14–16] Poor perfusion and reduced passive buffering capacity in the extracellular tumor microenvironment further exacerbates the decrease in tumor pH_e.[17,18] To better understand the mechanism of cellular internalization of nanoparticles at different pH values with dissipative particle dynamics simulations pH-responsive nano-sized drug delivery system that incorporated pH-sensitive polymers has recently been developed.[11,19]

Recently, selective targeting of acidic cancer cells without affecting normal cells has been demonstrated.[20,21] This method is based on application of a water-soluble membrane peptide **PHLIP-pH L**ow **I**nsertion **P**eptide, which acts as a nanosyringe. Acidic pH (<7.0) promotes the protonation of one or two aspartic residues in this peptide and it triggers the insertion of the pHLIP into the cell membrane, as well as the formation of a transmembrane alpha helix.[22] At neutral pH, the pHLIP peptide binds only weakly to the surface of the cell membrane, without insertion of the peptide.[23] pH-selective insertion and folding within membranes has been demonstrated to occur only in acidic tissues *in vivo*,[24,25] including in solid tumors (human and mouse).[26,27] Once inserted across the cell membranes within the acidic tissue, pHLIP remains in this state for a long period of time.[21,26] The affinity of the peptide for a lipid bilayer is about 20 times higher at acidic pHs (<7.0) than at higher pHs.[28]

It has been demonstrated in mice that the N-terminus of pHLIP when conjugated with various fluorescent probes or a ^{64}Cu-DOTA chelate that is used for PET imaging, can identify tumor sites and accumulate in tumor tissues of various types and at various stages of tumor development.[21,26] Ability of pHLIP to target tumors correlates with the aggressiveness of tumors: highly metastatic tumors, which are known to be more acidic[29] than non-metastatic ones are targeted much better by fluorescent pHLIP.[30] However, the shallow depth of tissue light penetration limits the use to endoscopy and optical imaging in

skin cancers. On the other hand, nuclear medicine techniques (such as PET or SPECT), although sensitive, are limited in their use due to lack of spatial resolution with respect to anatomical landmarks, and the short half-life of usable radioisotopes.

Magnetic resonance imaging (MRI) is a non-invasive and non-ionizing method that provides high spatial image resolution throughout the tissue. In addition, MRI method has no tissue penetration problem. Although there are many reports on pHLIP-tagged fluorescent and radiotracer imaging probes, no pHLIP-conjugated MRI probes have been reported. We have recently developed dendrimer-based pH-responsive MRI nanoprobe.[31,32] This paramagnetic nanoparticle is an attractive foundation for the development of a broadly useful, “smart” nanoparticle platform for both targeted acidic tumor imaging and drug delivery. This platform might easily accommodate targeting ligands for selective localization at the acidic tumor microenvironment as well as the therapeutic drugs that can be released selectively into tumor cells. Therefore, we investigated the pHLIP-tagged dendrimer-based pH-responsive paramagnetic nanoparticles in targeting cancer cells based on a physiological characteristic of tumor microenvironment. To monitor intracellular internalization and trafficking of paramagnetic nanoparticle, we also conjugated the fluorescent dye to the nanostructure.

We have synthesized a pH-responsive paramagnetic nanoparticle using our previously published synthetic methods.[32] The particle corresponds to a G5-dendrimer with an average of 44 chelated GdDOTA-4AmP^{5-} ions per dendrimer. In this report, Gd_{44}-G5 dendrimer was reacted with a heterobifunctional cross-linker, sulfosuccinimidyl 6-(3'-[2-pyridyldithio]-propionamido)hexanoate (sulfo-LC-SPDP) and then pyridinyldisulfide activated Gd_{44}-G5 dendrimer was coupled with a C-terminus cysteine group of biotinylated Bt-pHLIP (AEQNPIYWARYADWLFTTPLLLLDLALLVDADEGTCG-dpeg$_4$Biotin) (New England Peptide, Gardner, MA, USA) to form a disulfide bond. The conjugate was purified by diafiltration (C-10) to produce a final conjugate, Gd_{44}-G5-ss-Bt-pHLIP (Figure 1). A biotin molecule was attached to the C-terminus of pHLIP in order to quantify the number of pHLIP peptides conjugated with Gd_{44}-G5. The number of biotin molecules conjugated with PAMAM Gd_{44}-G5 dendrimer was determined using HABA-avidin assay (Pierce Chemical). The HABA assay with biotin and avidin revealed that on average 3.1 molecules of biotin were present in the Gd_{44}-G5-ss-Bt-pHLIP dendrimer. Since biotin was attached to the pHLIP peptide, an average of, 3.1 pHLIP peptides were also present in a Gd_{44}-G5-ss-Bt-pHLIP particle. Finally, rhodamine dye was conjugated to the surface amines of preloaded the Gd_{44}-G5-ss-Bt-pHLIP$_3$ in order to achieve the final conjugate Rho-Gd_{44}-G5-ss-Bt-pHLIP$_3$ as shown in Figure 1. Unreacted dye was removed by diafiltration (using C-10).

Free Gd^{3+} ions are toxic in vivo. To minimize toxicity Gd^{3+} ions are chelated with multidentate ligands to prevent tissue interaction and minimize toxic side effects. However, toxic Gd^{3+} ions may still be released in vivo by acid, competing endogenous metal ions such as zinc, calcium and copper or metabolism of the chelates. This report employed only macrocyclic chelates to tightly bind Gd^{3+}.[33] Macrocyclic chelates have significantly higher thermodynamic stability constants than linear chelates. Gd-DOTA-4AmP^{5-} is also kinetically more stable than that of acyclic Gd-DTPA.[34,35]

The exterior surface charge of this particle was assessed by zeta potential measurement. The surface charges of Gd_{44}-G5-Bt-$pHLIP_3$ at pH 7.4 and 6.5 were −34.21 ± 2.99 mV and − 2.41 ± 1.17 mV, respectively (Supplementary Figure S-1). This observation might be explained by the presence of 44 Gd-DOTA-4AmP^{5-} chelates on the surface of a G5 dendrimer. Gd-DOTA-4AmP^{5-} chelate has variable pK_a's ranging from 6.0 to 8.0.[35,34] Above the pK_a's, the chelate has −5 negative charge, while it has either neutral or positive charge below the pK_a's.[35] At acidic pH (<7.0), one or two aspartic residues in pHLIP become protonated. However, at neutral pH, both aspartic acid residues are at deprotonated state. Therefore, both Gd-DOTA-4AmP^{5-} chelate and pHLIP played a significant role in tuning the surface charge of the nanoparticle which is revealed by Zeta potential measurements (Supplementary Figure S-1).

To evaluate the ability of the peptide to translocate molecules across the cell membrane, we synthesized a version of biotinylated pHLIP with a single cysteine residue at its C terminus (AEQNPIYWARYADWLFTTPLLLLDLALLVDADEGTCG-($dpeg_4$Biotin) allowing it to be easily conjugated to pyridinyldisulfide-activated Gd_{44}-G5 through a sulphur-sulphur bond. To study pH- dependent translocation of molecules across the cell membrane, we added Rho-Gd_{44}-G5-ss-Bt-pHLIP to the cells and incubated them for 3h at a pH of either 7.4 or 6.5. The cells were then washed at pH 7.4 to remove any reversibly bound peptide. Rho-Gd_{44}-G5-ss-Bt-pHLIP did not exhibit any non-specific cellular up-take (Figure 2B), which might be attributed to the repulsive inter-action between the negatively charged cell membrane and negatively charged phosphonate-based Rho-Gd_{44}-G5-ss-Bt-pHLIP nanoparticles as evidenced by zeta potential measurement (Figure S-1).

The cellular membrane insertion of Rho-Gd_{44}-G5-$pHLIP_3$ was also tested by an *in vitro* MRI study at 7T using a Varian Direct- Drive MRI system (Figure 2E). Even incubation with a higher dose (15 mM) of contrast agent did not cause cell distress or toxicity, in agreement with previous reports.[36] Therefore, the design of an anionic dendrimeric version of MRI contrast agent aided in avoiding cell cytotoxicity. The cellular membrane binding of the nanoparticle was observed only for pHLIP-conjugated Rho-Gd_{44}-G5-ss-Bt-pHLIP at pH 6.5, as clearly demonstrated in Figure 2 (B, C, D) and 2E–F. Thus, we have shown the ability of pHLIP peptide for intracellular delivery of Rho-Gd_{44}-G5-ss-$pHLIP_3$ in vitro at pH 6.5 but the same ability was attenuated significantly at neutral pH or pH 7.4. Fluorescent microscopic imaging demonstrated the perinuclear fluorescence pattern (Figure 2F) indicating endosomal localization of the nanoparticles. The images were captured in live cells where we used LysoTracker to demonstrate co-localization of nanoparticles with endosomes/lysosomes after 2 h of incubation, as shown in Figure 3. Therefore, at lower pH (<7.0), Rho-Gd_{44}-G5-ss-$pHLIP_3$ was internalized into MDA-MB-231cells by the insertion of pHLIP where sulphur-sulphur bond between Gd44-G5 and pHLIP in the nanostructure was enzymatically cleaved upon trafficking into acidic endosomal or lysosomal subcellular compartments, resulting in a release of Rho-Gd44-G5 nanoparticle into the cytoplasm (Figure 2F). Several groups have also developed pHLIP-conjugated liposomes or polymers for conditional delivery of drugs and demonstrated the feasibility of releasing drugs inside endosomes/lysosomes.[37,38]

Cellular entry of Rho-Gd_{44}-G5-ss-Bt-$pHLIP_3$ was also evaluated by flow cytometry. Mesenchymal stem cells were used as a control (normal) cells. When these cells were incubated with Rho-Gd_{44}-G5-ss-Bt-$pHLIP_3$ flow cytometry did not show any fluorescence shift under both, pH 6.5 and 7.4 (Figure 4a). At the same time, three cancer cell lines, U251, MDA-MB-231 and U87, treated with the same nanoparticles exhibited a very low level of fluorescence shift at pH 7.4, due to low level of membrane attachment (red line in Figure 4 b to d). However, at pH 6.5, a new population of highly fluorescent cells was observed for all three cancer cell lines (blue line in Figure 4 b to d). We conclude that this dendrimeric platform can aid in intracellular delivering of therapeutic molecules that do not enter cells on their own.

In conclusion, we have demonstrated pH-responsive dual-mode optical/MRI contrast agent. pH-dependent cellular internalization of (Gd-DOTA-4AmP)$_{44}$-G5-ss-Bt-$pHLIP_3$ was evaluated by both *in vitro* MRI and microscopic fluorescence imaging. Finally, the platform can be applied in different aggressive acidic cancer types, and where no other prognostic factor is a reliable biomarker for response.

Supplementary Material

Refer to Web version on PubMed Central for supplementary material.

Acknowledgments

The authors acknowledge research support from NIH grant (R01 CA206190) to M.M.A.

Reference

1. Srinivas PR, Kramer BS, Srivastava S. Trends in biomarker research for cancer detection. The lancet oncology. 2001; 2(11):698–704. [PubMed: 11902541]
2. Hanke JH, Webster KR, Ronco LV. Protein biomarkers and drug design for cancer treatments. Eur J Cancer Prev. 2004; 13(4):297–305. [PubMed: 15554558]
3. Bild AH, Yao G, Chang JT, et al. Oncogenic pathway signatures in human cancers as a guide to targeted therapies. Nature. 2006; 439(7074):353–357. [PubMed: 16273092]
4. Poon Z, Chang D, Zhao X, Hammond PT. Layer-by-layer nanoparticles with a pH-sheddable layer for in vivo targeting of tumor hypoxia. ACS nano. 2011; 5(6):4284–4292. [PubMed: 21513353]
5. Shenoy D, Little S, Langer R, Amiji M. Poly(ethylene oxide)-modified poly(beta-amino ester) nanoparticles as a pH-sensitive system for tumor-targeted delivery of hydrophobic drugs: part 2. In vivo distribution and tumor localization studies. Pharmaceutical research. 2005; 22(12):2107–2114. [PubMed: 16254763]
6. Shenoy D, Little S, Langer R, Amiji M. Poly(ethylene oxide)-modified poly(beta-amino ester) nanoparticles as a pH-sensitive system for tumor-targeted delivery of hydrophobic drugs. 1. In vitro evaluations. Molecular pharmaceutics. 2005; 2(5):357–366. [PubMed: 16196488]
7. Devalapally H, Shenoy D, Little S, Langer R, Amiji M. Poly(ethylene oxide)-modified poly(beta-amino ester) nanoparticles as a pH-sensitive system for tumor-targeted delivery of hydrophobic drugs: part 3. Therapeutic efficacy and safety studies in ovarian cancer xenograft model. Cancer chemotherapy and pharmacology. 2007; 59(4):477–484. [PubMed: 16862429]
8. Warburg O. On the origin of cancer cells. Science. 1956; 123(3191):309–314. [PubMed: 13298683]
9. Wike-Hooley JL, Haveman J, Reinhold HS. The relevance of tumour pH to the treatment of malignant disease. Radiotherapy and oncology : journal of the European Society for Therapeutic Radiology and Oncology. 1984; 2(4):343–366. [PubMed: 6097949]

10. Griffiths JR. Are cancer cells acidic? British journal of cancer. 1991; 64(3):425–427. [PubMed: 1911181]
11. Ding HM, Ma YQ. Controlling cellular uptake of nanoparticles with pH-sensitive polymers. Sci. Rep. 2013; 3:2804. [PubMed: 24076598]
12. Griffiths JR, McIntyre DJ, Howe FA, Stubbs M. Why are cancers acidic? A carrier-mediated diffusion model for H+ transport in the interstitial fluid. Novartis Foundation symposium. 2001; 240:46–62. discussion 62-47, 152–153. [PubMed: 11727936]
13. Schornack PA, Gillies RJ. Contributions of cell metabolism and H+ diffusion to the acidic pH of tumors. Neoplasia. 2003; 5(2):135–145. [PubMed: 12659686]
14. Terpstra M, High WB, Luo Y, de Graaf RA, Merkle H, Garwood M. Relationships among lactate concentration, blood flow and histopathologic profiles in rat C6 glioma. NMR in biomedicine. 1996; 9(5):185–194. [PubMed: 9067999]
15. Walenta S, Wetterling M, Lehrke M, et al. High lactate levels predict likelihood of metastases, tumor recurrence, and restricted patient survival in human cervical cancers. Cancer research. 2000; 60(4):916–921. [PubMed: 10706105]
16. Schwickert G, Walenta S, Sundfor K, Rofstad EK, Mueller-Klieser W. Correlation of high lactate levels in human cervical cancer with incidence of metastasis. Cancer research. 1995; 55(21):4757–4759. [PubMed: 7585499]
17. Jain RK. Determinants of tumor blood flow: a review. Cancer research. 1988; 48(10):2641–2658. [PubMed: 3282647]
18. Bhujwalla ZM, Aboagye EO, Gillies RJ, Chacko VP, Mendola CE, Backer JM. Nm23-transfected MDA-MB-435 human breast carcinoma cells form tumors with altered phospholipid metabolism and pH: a 31P nuclear magnetic resonance study in vivo and in vitro. Magnetic resonance in medicine : official journal of the Society of Magnetic Resonance in Medicine / Society of Magnetic Resonance in Medicine. 1999; 41(5):897–903.
19. Ding HM, Ma YQ. Theoretical and computational investigations of nanoparticle-biomembrane interactions in cellular delivery. Small. 2015; 11(9–10):1055–1071. [PubMed: 25387905]
20. Andreev OA, Reshetnyak YK. Mechanism of formation of actomyosin interface. Journal of molecular biology. 2007; 365(3):551–554. [PubMed: 17081565]
21. Reshetnyak YK, Andreev OA, Lehnert U, Engelman DM. Translocation of molecules into cells by pH-dependent insertion of a transmembrane helix. Proceedings of the National Academy of Sciences of the United States of America. 2006; 103(17):6460–6465. [PubMed: 16608910]
22. Andreev OA, Engelman DM, Reshetnyak YK. Targeting acidic diseased tissue: New technology based on use of the pH (Low) Insertion Peptide (pHLIP). Chimica oggi. 2009; 27(2):34–37. [PubMed: 20037661]
23. Andreev OA, Engelman DM, Reshetnyak YK. pH-sensitive membrane peptides (pHLIPs) as a novel class of delivery agents. Molecular membrane biology. 2010; 27(7):341–352. [PubMed: 20939768]
24. Macholl S, Morrison MS, Iveson P, et al. In vivo pH imaging with (99m)Tc-pHLIP. Molecular imaging and biology : MIB : the official publication of the Academy of Molecular Imaging. 2012; 14(6):725–734. [PubMed: 22371188]
25. Sosunov EA, Anyukhovsky EP, Sosunov AA, et al. pH (low) insertion peptide (pHLIP) targets ischemic myocardium. Proceedings of the National Academy of Sciences of the United States of America. 2013; 110(1):82–86. [PubMed: 23248283]
26. Vavere AL, Biddlecombe GB, Spees WM, et al. A novel technology for the imaging of acidic prostate tumors by positron emission tomography. Cancer research. 2009; 69(10):4510–4516. [PubMed: 19417132]
27. Yao L, Daniels J, Moshnikova A, et al. pHLIP peptide targets nanogold particles to tumors. Proceedings of the National Academy of Sciences of the United States of America. 2013; 110(2): 465–470. [PubMed: 23267062]
28. Zoonens M, Reshetnyak YK, Engelman DM. Bilayer interactions of pHLIP, a peptide that can deliver drugs and target tumors. Biophysical journal. 2008; 95(1):225–235. [PubMed: 18359793]
29. Gillies RJ, Schornack PA, Secomb TW, Raghunand N. Causes and effects of heterogeneous perfusion in tumors. Neoplasia. 1999; 1(3):197–207. [PubMed: 10935474]

30. Reshetnyak YK, Yao L, Zheng S, Kuznetsov S, Engelman DM, Andreev OA. Measuring tumor aggressiveness and targeting metastatic lesions with fluorescent pHLIP. Molecular imaging and biology : MIB : the official publication of the Academy of Molecular Imaging. 2011; 13(6):1146–1156. [PubMed: 21181501]

31. A B, R K, N R, Meza V, Morelatto R, Piccinni D. [Malignant melanoma of the oral cavity]. Rev Fac Cien Med Univ Nac Cordoba. 2008; 65(2):70–73. [PubMed: 20803941]

32. Bhuiyan MP, Aryal MP, Janic B, et al. Concentration-independent MRI of pH with a dendrimer-based pH-responsive nanoprobe. Contrast media & molecular imaging. 2015; 10(6):481–486. [PubMed: 26173742]

33. Sherry AD, Caravan P, Lenkinski RE. Primer on gadolinium chemistry. Journal of magnetic resonance imaging : JMRI. 2009; 30(6):1240–1248. [PubMed: 19938036]

34. Kalman FK, Baranyai Z, Toth I, et al. Synthesis, potentiometric, kinetic, and NMR Studies of 1,4,7,10-tetraazacyclododecane-1,7-bis(acetic acid)-4,10-bis(methylenephosphonic acid) (DO2A2P) and its complexes with Ca(II), Cu(II), Zn(II) and lanthanide(III) ions. Inorganic chemistry. 2008; 47(9):3851–3862. [PubMed: 18380456]

35. Kalman FK, Woods M, Caravan P, et al. Potentiometric and relaxometric properties of a gadolinium-based MRI contrast agent for sensing tissue pH. Inorganic chemistry. 2007; 46(13): 5260–5270. [PubMed: 17539632]

36. Drake FT, Van Eaton EG, Huntington CR, Jurkovich GJ, Aarabi S, Gow KW. ACGME case logs: Surgery resident experience in operative trauma for two decades. The journal of trauma and acute care surgery. 2012; 73(6):1500–1506. [PubMed: 23188243]

37. Zhao Z, Meng H, Wang N, et al. A controlled-release nanocarrier with extracellular pH value driven tumor targeting and translocation for drug delivery. Angew Chem Int Ed Engl. 2013; 52(29):7487–7491. [PubMed: 23757374]

38. Yao L, Daniels J, Wijesinghe D, Andreev OA, Reshetnyak YK. pHLIP(R)-mediated delivery of PEGylated liposomes to cancer cells. Journal of controlled release : official journal of the Controlled Release Society. 2013; 167(3):228–237. [PubMed: 23416366]

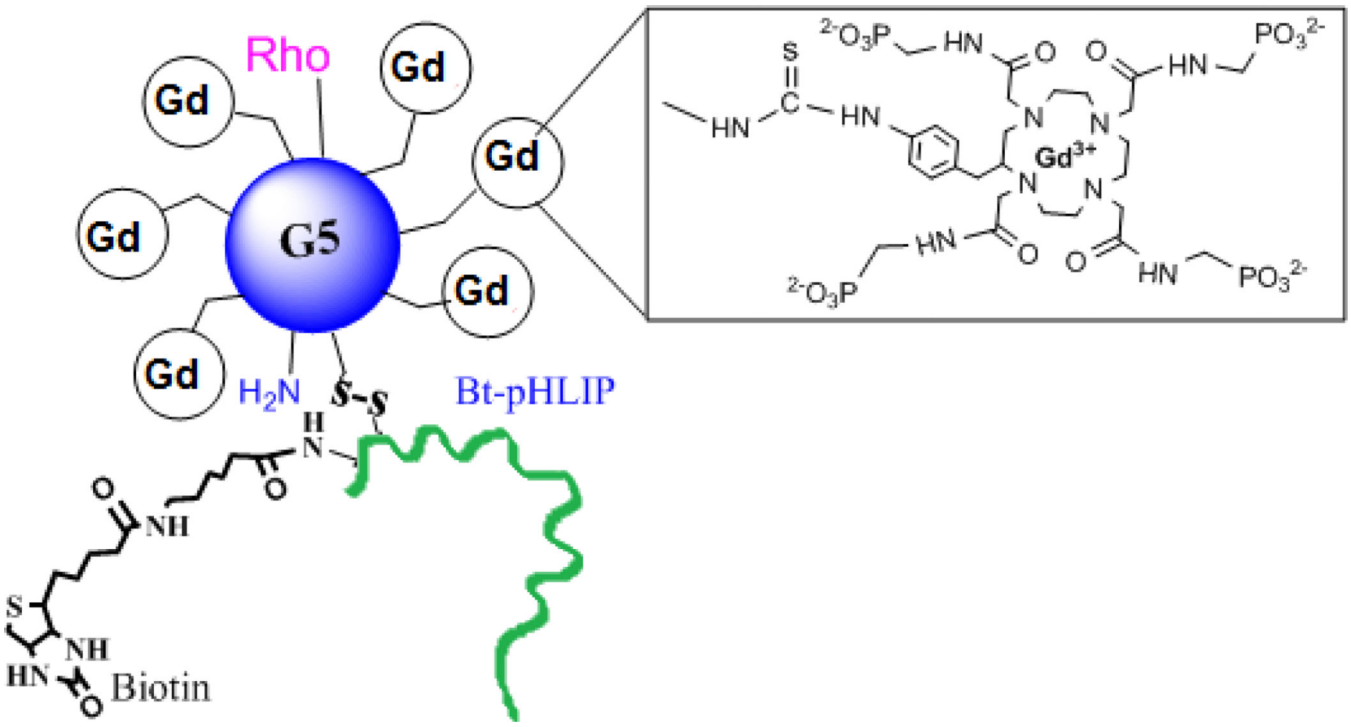

Figure 1.

Schematic view of Gd^{3+} chelated with 1,4,7,10-tetraaza-cyclododecane-1,4,7,10-tetraaminophosphonate (DOTA-4AmP^{8-}) in a Gd_{44}-G5 PAMAM dendrimer with rhodamine (Rho) and Bt-pHLIP conjugation. Gd_{44}-G5 is linked with Bt-pHLIP through sulphur-sulphur bond.

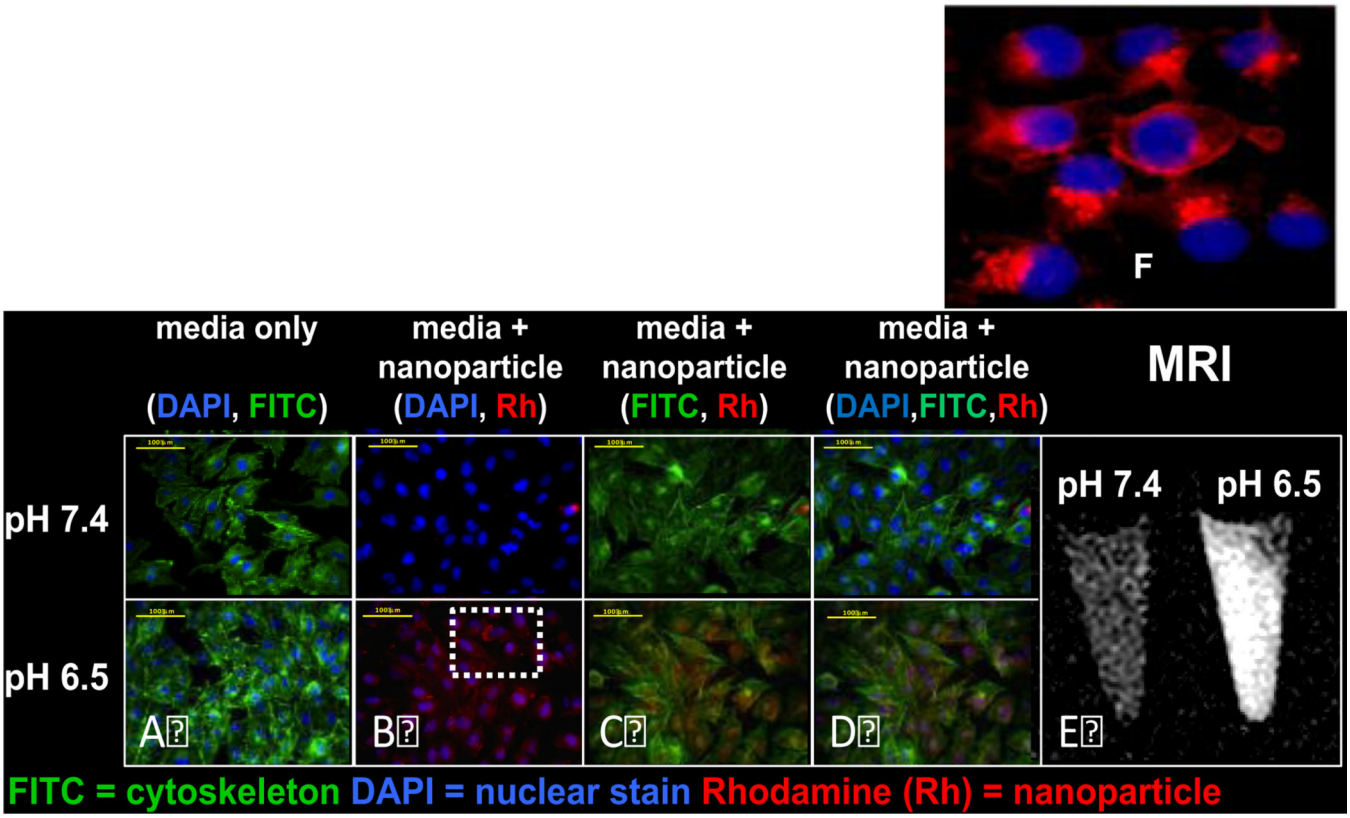

Figure 2.

In vitro fluorescence microscopy of MDA-MB-231 cells incubated for 3 hours in media containing rhodamine B conjugated Gd_{44}-G5-$pHLIP_3$ dendrimer at pH 7.4 and at pH 6.5 at a concentration of 7.1 μM with respect to rhodamine B. Nuclei were visualized with DAPI (blue fluorescence). Cyto-skeleton was visualized by FITC CytoPainter F-Actin specific dye (green fluorescence). Intracellular uptake was visualized by red fluorescence of Rhodamine conjugated to the nanoparticle (see **B**). Scale bars = 100 μm. Panel **A** showing cells incubated in media only. Images of cells incubated in the presence of media and nanoparticle were captured using DAPI and Rh filters (**B**), FITC and Rh filters (**C**) and DAPI, FITC and Rh filters (**D**). Cytoskeleton was visualized by FITC Cyto-Painter F-Actin specific dye. **Panel 2E:** *In-vitro* NP specificity quantified by MRI. T1- maps of gel phantoms containing MDA-MB-231 cells incubated with NP at pH 6.5 and 7.4. **Panel 2F:** Enlarged image of perinuclear distribution of Rho-Gd_{44}-G5-ss-$pHLIP_3$ from overlaid images of dapi and nanoparticle (**B**).

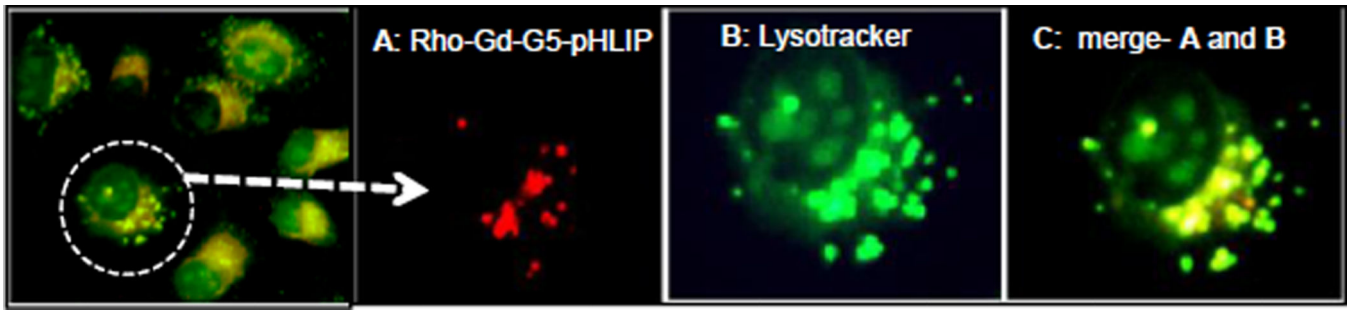

Figure 3.

In vitro fluorescence microscopy images of MDA-MB-231 live cell incubated for 2 hours in media containing rhodamine B conjugated Gd-G5—ss-Bt-pHLIP$_3$ dendrimer at pH 6.5. Nano-particle is red (**A**) and lysotracker green, detecting endosomes and lysosomes is shown in green (**B**). Overlay between (**A**) and (**B**) is represented in yellow (**C**). Overlaid images are shown in the far left and far right panel.

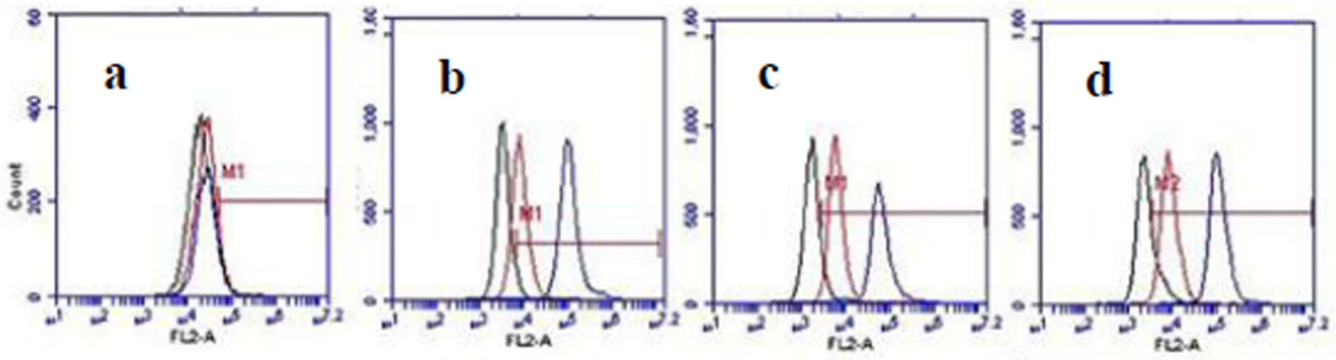

Figure 4.

Flow cytometry of the cell entry dynamics of Rho-Gd_{44}-G5-ss-Bt-$pHLIP_3$ conjugate (particle is attached to C-terminus of the peptide) in **MSC (a)** (mesenchymal stem cell), **U251 (b), MDA-MB-231 (c)** and **U87 (d)** cell lines. The log of rhodamine adsorption intensity (FL1-H on X axis is plotted against the number of cells (counts on y axis). No cellular uptake of the nanoparticle in normal **MSC (a)** was observed for both pH (6.5 and 7.4). In contrast, the cellular uptake of the nanaoparticle in all three cancer cell lines (**b, c & d**) is evident at lower pH 6.5. (black line) Control (no probe at pH 7.4); (red line) nanoparticle at pH 7.4; (blue line) nanoparticle at pH 6.5.